Environmental Impact Assessment Review 75 (2019) 13–26

Contents lists available at ScienceDirect

Environmental Impact Assessment Review

journal homepage: www.elsevier.com/locate/eiar

Can groundwater vulnerability models assess seawater intrusion?

Momejian N.[a,b], Abou Najm M.[a,c], Alameddine I.[a], El-Fadel M.[a,*]

[a] Department of Civil & Environmental Engineering, American University of Beirut, Lebanon
[b] Department of Geography and Planning, Queen's University, Kingston, Ontario, Canada
[c] Department of Land, Air, and Water Resources, University of California, Davis, California, United States

ARTICLE INFO

Keywords:
Groundwater vulnerability
Seawater intrusion
DRASTIC
EPIK

ABSTRACT

This study examines the uncertainty associated with two commonly used GIS-based groundwater vulnerability models, *DRASTIC* and *EPIK*, in assessing seawater intrusion, a growing threat along coastal urban areas due to overexploitation of groundwater resources. For this purpose, concentrations of Total Dissolved Solids (TDS) in groundwater samples at three pilot areas along the Eastern Mediterranean were compared with mapped vulnerability predictions obtained through *DRASTIC* and *EPIK*. While field measurements demonstrated high levels of groundwater salinity depending on the density of urbanization, both vulnerability assessment methods exhibited a limited ability in capturing saltwater intrusion dynamics. In the three pilot areas, DRASTIC was only able to predict correctly between 8.3 and 55.6% of the salinity-based water quality ranges, while EPIK's predictions ranged between 11.7 and 77.8%. This emphasizing that conventional vulnerability models perform poorly when anthropogenic impacts induce lateral flow processes such as seawater intrusion caused primarily by vertical groundwater extraction.

1. Introduction

The vulnerability of groundwater to seawater intrusion is increasing as a result of unsustainable extraction practices along coastal urban areas, where population growth and development have induced groundwater overexploitation exceeding the natural recharge (Chang, 2010; Howard, 2002; Tabatabaei et al., 2014). Groundwater vulnerability is further accentuated with the decrease in infiltration and recharge capacities caused by land use and land cover changes associated with urbanization (IPCC, 2013; Michalopoulos and Dimitriou, 2018). It is also expected to exacerbate with sea level rise under potential future climate change. The latter affects the components of the water cycle as well (increased temperature and evaporation, change in spatial and temporal precipitation patterns), which may further increase net water demand and hinder groundwater recharge (Fetter, 2001; Howard, 2002; Loáiciga et al., 2012; Ranjan et al., 2006; Vorosmarty et al., 2000; Werner et al., 2012).

Aquifer vulnerability, defined as aquifer sensitivity to various stresses (climatic or anthropogenic), was first used to evaluate the potential exposure of aquifers to contaminants (Magiera, 2000; Vlaicu and Munteanu, 2008). Several groundwater vulnerability assessment (GVA) models have been developed to provide insight on groundwater conditions based on physical parameters of the medium containing the groundwater. The medium is usually a static system that varies only over geological time spans. Assessments using these models are mostly based on the intrinsic characteristics of the groundwater bearing formations (aquifers), including geology, geomorphology, and hydrogeology (Fijani et al., 2013; Vlaicu and Munteanu, 2008). They also account for the layers that affect these formations including soil cover, land use, topography, and hydrology (Stigter et al., 2005; Yang et al., 2017). The models usually adopt an Index and Overlay (IO) system to generate scores based on ranks or weights that are assigned to the intrinsic parameters. Most models produce a dimensionless value that is referred to as the total vulnerability that can vary spatially in 2D; yet they lack a vertical component (Elewa et al., 2013; Gogu and Dassargues, 2000a; Milnes, 2011; Shirazi et al., 2012).

Most GVA models are reportedly suitable for data-scarce regions (Panagopoulos et al., 2006; Vlaicu and Munteanu, 2008) and are invariably coupled with Geographic Information Systems (GIS) to provide decision makers with informative visualization of complex groundwater systems to aid in the decision-making process towards protecting aquifers from pollution risk (Kazakis et al., 2015). Recent attempts have focused on adding to the modeling framework new external factors such as contaminant source and type, climate change forcings, and/or other regional impacts (Ahmadian, 2013; Fijani et al., 2013; Shirazi et al., 2012; Rangel-Medina et al., 2004). While such tools have often been

* Corresponding author.
E-mail address: mfadel@aub.edu.lb (M. El-Fadel).

https://doi.org/10.1016/j.eiar.2018.10.003
Received 11 July 2018; Received in revised form 13 September 2018; Accepted 6 October 2018
Available online 27 November 2018

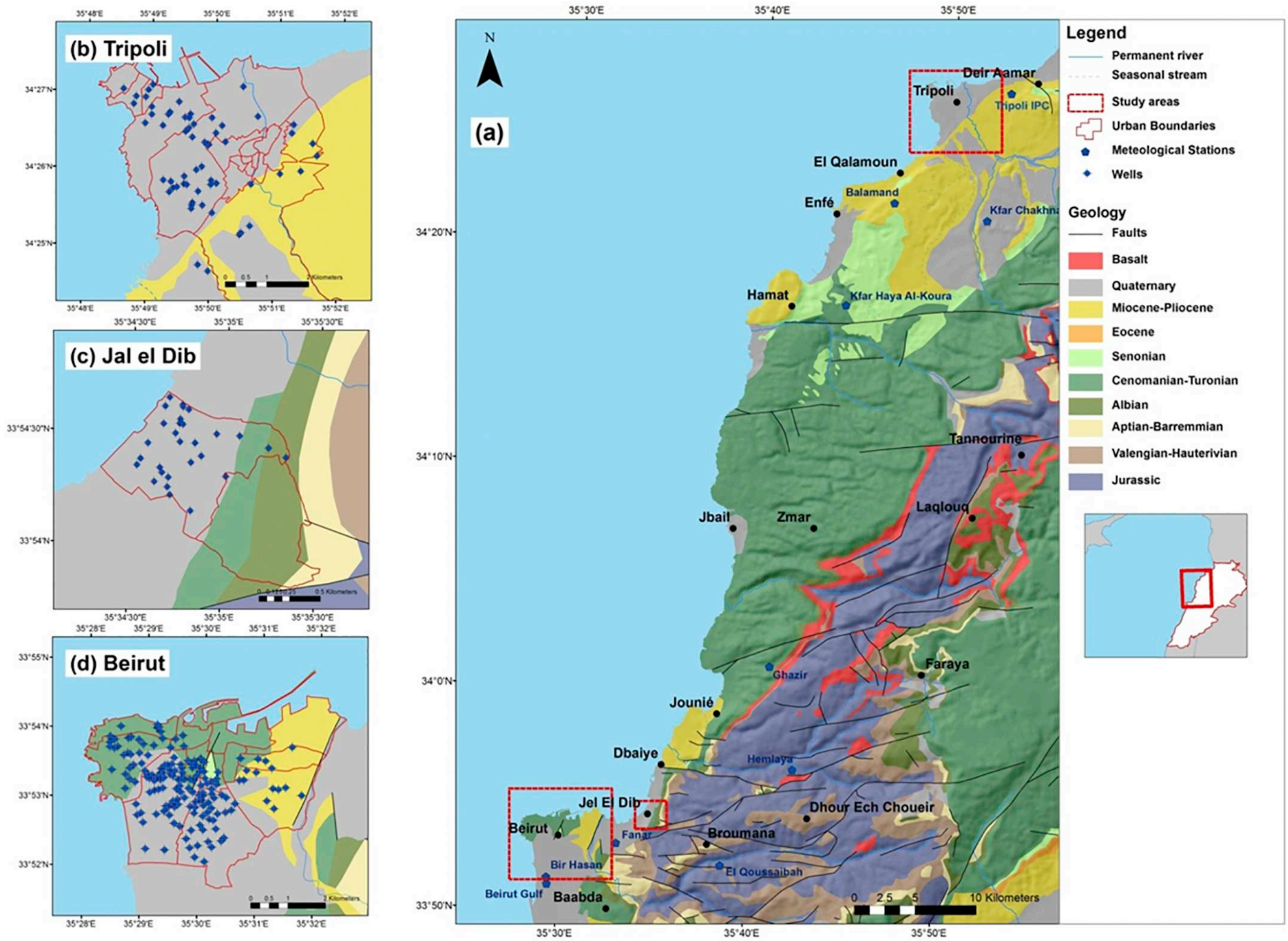

Fig. 1. General location of the study area with location of sampling wells. (a) Geological formations (b) Tripoli (c) Jal el Dib (d) Beirut.

reported to improve decision-making, they have also been criticized of being unreliable given their inability to recognize the complexity of the system (Focazio, 2002; Neukum et al., 2008) and their tendency to generalize on assumptions (Gogu and Dassargues, 2000a; Doerfliger et al., 1999). As such, in this study, two commonly used GVA models were tested to evaluate and compare their ability in assessing groundwater vulnerability to seawater intrusion. Vulnerability maps were generated and combined with results from a groundwater quality-monitoring program to assess the ability of the models in identifying the vulnerability of coastal aquifers under the stress of seawater intrusion induced by groundwater overexploitation (Kaliraj et al., 2015; Tabatabaei et al., 2014).

2. Materials and methods

2.1. Study area characteristics

The GVA models targeted three pilot areas representing the Lebanese coastal cities of Beirut (628,000 people and 22 km^2), Jal el Dib (40,000 people and 1.5 km^2), and Tripoli (400,000 people and 11 km^2) (Fig. 1) along the Eastern Mediterranean coastline (Awad and Darwich, 2009; El-Fadel et al., 2003). The three cities experience mild wet winters (< 1000 ml of precipitation) and hot dry summers (average 22 °C) (Meteorological Center, 1977). Similar to many coastal cities along the Mediterranean (De Filippis et al., 2016; Marin et al., 2010a,b), the three pilot areas are underlain by karstic and semi-karstic aquifer systems of Jurassic and Cretaceous age up until quaternary age deposits (Dubertret, 1955; Walley, 1997). These aquifers constitute the main groundwater sources and cover > 70% of the country (Edgell, 1997), particularly along the coast, where nearly 80% of the population resides (Central Administration of Statistics, 2009). The water supply at all pilot aquifers is often complemented with groundwater extracted mostly through a large number of unlicensed wells pumping at different intensities to alleviate chronic water shortages, particularly during the dry season. Groundwater sampling campaigns were conducted towards the end of the summer season to assess the extent of seawater intrusion under worst-case conditions. Thirty wells were sampled in Jal el Dib, 60 in Tripoli, and 165 in Beirut (El-Fadel et al., 2014a,b). The samples

Table 1
Comparison of commonly used intrinsic vulnerability assessment methods with corresponding parameter.

	Generic			*Karst aquifers*			*Lateral contaminant*	*Site specific*
Included parameter	*DRASTIC*[a]	*SINTACS*[b]	*GOD*[e]	*EPIK*[c]	*COP + K*[d]	*PI*[f]	*GALDIT*[g]	*WMCDSS*[h]
Precipitation/recharge rate/water balance	X	X		X	X	X	–	X
Vadose (unsaturated) zone	X	X	X	X	X	X	–	–
Aquifer/lithology /hydrogeological characteristics	X	X	X	X	X	X	–	–
Soil	X	X	X	X	X	X	–	–
Topography	X	X	–	X	X	X	–	–
Hydraulic conductivity	X	X	–	X	X	–	X	X
Land Use	–	X	–	X	X	X	–	–
Distance from shoreline	–		–	–			X	–

[a] DRASTIC (Depth to Water (D), Recharge (R), Aquifer Media (A), Soil Media (S), Topography (T), Impact of Vadose zone (I), Conductivity (C)): e.g. Ahirwar and Shukla, 2018; Ahmed et al., 2017; Aller et al., 1987; Allouche et al., 2017; Al-Rawabdeh et al., 2014; Baalousha, 2016; Bartzas et al., 2017; Boufekane and Saighi, 2018; Colins et al., 2016; Ghazavi and Ebrahimi, 2015; Hammouri and El-Naqa, 2008; Haque et al., 2018; Jamrah et al., 2008; Jarray et al., 2017; Kaliraj et al., 2015; Kaliraj et al., 2015; Kardan Moghaddam et al., 2017; Kazakis et al., 2015; Khakhar et al., 2017; Kumar et al., 2014; Kumar et al., 2017; Kura et al., 2015; Lasagna et al., 2018; Mahmoudzadeh et al., 2013; Michalopoulos and Dimitriou, 2018; Nadiri et al., 2017; Nadjai et al. 2017; Neukum et al., 2008; Oroji and Karimi, 2018; Panagopoulos et al., 2006; Sadat-Noori and Ebrahimi, 2016; Saidi et al., 2014; Shirazi et al., 2012; Sinha et al., 2016; Tabatabaei et al., 2014; Tiwari et al., 2016; Neh et al., 2015; Vlaicu and Munteanu, 2008; Yang et al., 2017; Yin et al., 2013.

[b] SINTACS (Water table depth (S), Effective infiltration (I), Unsaturated zone (N), Soil media (T), Aquifer media (A), Hydraulic conductivity zone (C), Topographic slope (S)): e.g. Gogu et al., 2003;Kumari et al., 2016; Loborec et al., 2015; Polemio et al., 2009; Rangel-Medina et al., 2004; Vlaicu and Munteanu, 2008.

[c] EPIK (Epikarst (E) Protective Cover (P), Infiltration condition (I), Karst network development (K)): e.g. Awawdeh and Nawafleh, 2008; Baalousha, 2016; Barrocu et al., 2006; Doerfliger, 1996; Doerfliger et al., 1999; Gogu and Dassargues, 2000b; Hamdan et al., 2016; Hammouri and El-Naqa, 2008; Kazakis et al., 2015; Loborec et al., 2015; Neukum et al., 2008; Pera and Valcarce, 2009; Polemio et al., 2009; Rangel-Medina et al., 2004; Ravbar and Goldscheider, 2009; SAEFL, 1998; Vlaicu and Munteanu, 2008.

[d] COP or COP + K (Control the flow concentration (C), protective capacity of the Overlying layers by means of soils (O), Precipitation (P), the groundwater travel time, the connection and contribution to the source, as well as the active conduit network (K)): e.g. Hamdan et al., 2016; Loborec et al., 2015; Marín et al., 2010b; Michalopoulos and Dimitriou, 2018; Polemio et al., 2009; Rangel-Medina et al., 2004; Vlaicu and Munteanu, 2008.

[e] GOD (groundwater occurrence (G). overall aquifer class (0), depth to groundwater (D)): Ghazavi and Ebrahimi, 2015; Gogu et al., 2003;Lasagna et al., 2018; Mahmoudzadeh et al., 2013; Polemio et al., 2009; Rangel-Medina et al., 2004; Vlaicu and Munteanu, 2008.

[f] *PI* (protective cover (P), infiltration conditions (I)): e.g. Goldscheider, 2005; Neukum et al., 2008; Polemio et al., 2009; Rangel-Medina et al., 2004; Ravbar and Goldscheider, 2009; Vlaicu and Munteanu, 2008.

[g] GALDIT (Groundwater occurrence (G), Aquifer hydraulic conductivity (A), Depth to groundwater level above sea (L), Distance from the shore (D), Impact of existing status of seawater intrusion in the area (I), Thickness of the aquifer which is being mapped (T)): Allouche et al., 2017; Chachadi and Lobo-Ferreira, 2005; Chachadi and Lobo-Ferreira, 2001; Kardan Moghaddam et al., 2017; Kura et al., 2015; Saidi et al., 2014.

[h] WMCDSS (weighted (W) multi-criteria (MC) decision (D) support (S) system (S)): Elewa et al., 2013.

were transported on ice to the Environmental Engineering Research Center at the American University of Beirut and analyzed for various physical and biochemical indicators in accordance with *Standard Methods for the Examination of Water and Wastewater* (APHA/AWWA/WEF, 2012). In this study, only total dissolved solids (TDS) levels were used as a salinity indicator.

2.2. GVA Model Selection

Common GVA models vary in their ability to account for potential contamination (Chachadi and Lobo-Ferreira, 2001; Elewa et al., 2013; Hao et al., 2017; Rangel-Medina et al., 2004; Selmi, 2013). Models designed specifically for surface contamination have been equally used for non-vertical contamination (Chachadi and Lobo-Ferreira, 2005; Elewa et al., 2013; Selmi, 2013); sometimes through modifications to account for non-vertical pollution sources (Jamrah et al., 2008). Table 1 presents a summary of commonly used intrinsic vulnerability assessment methods and their corresponding parameters, excluding the models that are specifically designed for agricultural areas such as the SEEPAGE (Kumar et al., 2015) or DRASTIC-LU/DRASTIC-L (Alam et al., 2014; Sinha et al., 2016; Stigter et al., 2005; Yang et al., 2017) or DRASTIC-FM (Kazakis et al., 2015). *DRASTIC* appears as one of the most commonly used GVA. It was designed for large areas and applied over several aquifer types (porous-karstic-mixed) (e.g. Baalousha, 2016; Fijani et al., 2013; Kallioras et al., 2011; Kazakis et al., 2015; Khan et al., 2010; Michalopoulos and Dimitriou, 2018; Metni et al., 2004; Neukum et al., 2008; Panagopoulos et al., 2006; Sadat-Noori and Ebrahimi, 2016; Salemi et al., 2011; Shirazi et al., 2012; Werner et al., 2012). *SINTACS* and *PI* are equally comprehensive with respect to the number of parameters they include but they are not as commonly used (Kumari et al., 2016). *WMCDSS* is reportedly a highly site-specific model; yet it has been shown to be difficult to transfer between regions (Elewa et al., 2013). *EPIK*, *COP + K* and the *PI* models are GVAs that have been developed to account for karstic aquifers (Baalousha, 2016; Gogu and Dassargues, 2000b; Goldscheider, 2005; Hamdan et al., 2016; Polemio et al., 2009; Vlaicu and Munteanu, 2008; Voigt et al., 2004). The COP + K is an intrinsic vulnerability mapping used for karstic aquifer catchment areas; it was approved by the Pan-European COST Action 620. The model is a modification of the COP method (Vías et al., 2006) for karstic environments (Andreo et al. 2006; Jiménez-Madrid et al. 2010). COP and COP + K were applied on several Mediterranean karst springs (Hamdan et al., 2016; ELARD, 2015; Masoompour Samakosh et al. 2013; Andreo et al. 2006; Vías et al., 2006). Their results were found to be comparable to those generated by EPIK (Hamdan et al., 2016; Loborec et al., 2015). The *GOD* model is used mostly in regions where vulnerability variations are large within a small area

Fig. 2. *DRASTIC* with weights and ranks for model parameters.
Based on relative importance (Aller et al., 1987;Metni et al., 2004).
SS = Sandstone, LS = Limestone, weathrd = weathered, Meta. & metamor. = metamorphic, ign. = igneous.
Note that the depth to groundwater at the three pilot areas exhibit minimal fluctuations due to limited topographic changes coupled with coastal proximity inducing seawater-freshwater interaction that maintain a relatively constant groundwater level.
Units: Depth to Water (1 ft = 0.3048 m); Net Recharge (1 in. = 25.4 mm); Hydraulic Conductivity (1 GDP/ft^2 = 0.0408 m/day).

(Ahmed et al., 2017; Polemio et al., 2009). The *GALDIT* and *WMCDSS* models have not been adequately tested in a karstic environment (Allouche et al., 2017; Chachadi and Lobo-Ferreira, 2005; Chachadi et al., 2002; Chachadi and Lobo-Ferreira, 2001; Elewa et al., 2013; Kallioras et al., 2011; Kardan Moghaddam et al., 2017; Kura et al., 2015; Lobo-Ferreira et al., 2007; Najib et al., 2012; Saidi et al., 2014; Selmi, 2013). In this study, the performance of the generalized vulnerability model (*DRASTIC*) was evaluated along with a karst-specific vulnerability model (*EPIK*) (Baalousha, 2016; Doerfliger et al., 1999; Hammouri and El-Naqa, 2008; Kazakis et al., 2015; Kumar et al., 2015; Neukum et al., 2008) to compare their skill in assessing groundwater vulnerability to seawater intrusion. The models' selection criteria focused on choosing models that have been used in similar geologies, with at least one method developed for karstic systems, and those that have a limited set of input data requirements since the study area is characterized with data-scarcity.

DRASTIC is an intrinsic GVA model that uses IO of seven parameters (Fig. 2) to assess the vulnerability of an aquifer to groundwater contamination. It was developed for the US Environmental Protection Agency (EPA) and is reportedly suitable for porous/granular aquifers at a large scale (Aller et al., 1987). Each parameter is assigned a weight (W = 1 to 5) relative to its impact on the aquifer vulnerability and each sub-category within one parameter is rated (R = 1 to 10) based on its influence on the parent parameter. The model generated a *DRASTIC*

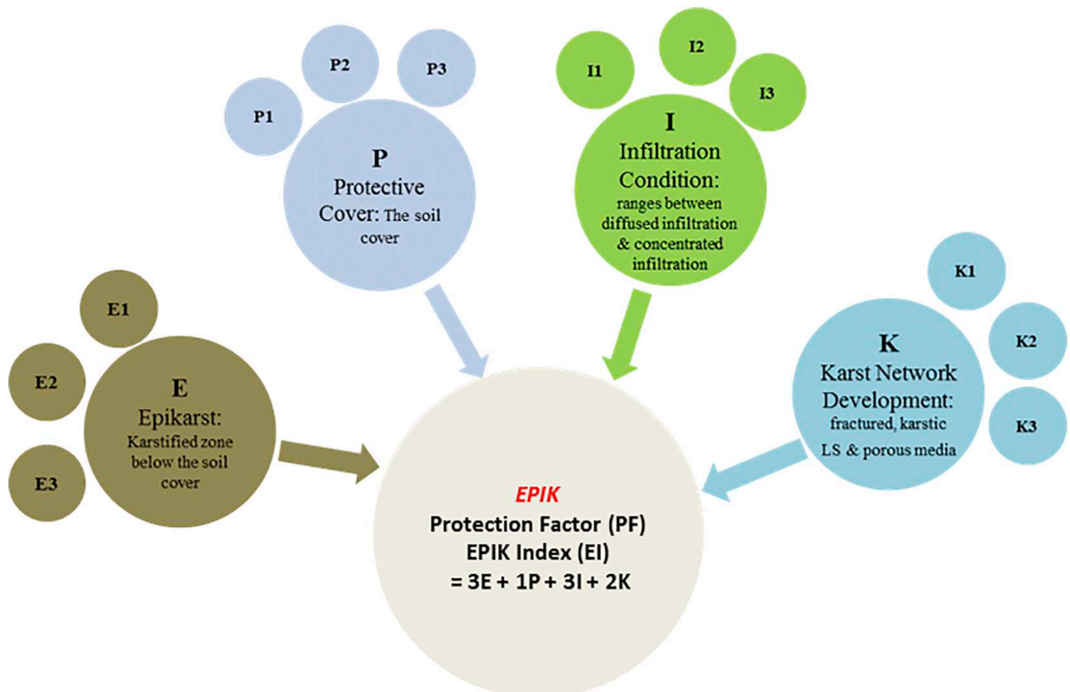

Fig. 3. *EPIK* with weights and ranks for model parameters.
*Detailed description presented in*Table 2.

Table 2
Definitions and scoring system for the three tested EPIK modifications with urban areas factor as main variation.

Parameter	*V1*	*V2*	*V3*	*Weight/rank*
Epikarst				*3*
E1	Fractures, developed faults, current/paleo channels/Rivers, flood plains + Buffer (500 m) around faults + Buffer 500 m around Rivers	Same as V1	Same as V1	2
E2	Karst outcropping formations	Same as V1	Same as V1	3
E3	The rest of the area with absent karstic morphology	Same as V1	Same as V1	4
Protective Cover				*1*
P1	No protective cover	Same as V1	No protective cover + *urban*	1
P2	Quaternary cover + dynamic buffer to an elevation of 100 m asl on the coastline*	Same as V1	Same as V1	2
P3	500 m buffer around rivers channels	Same as V1	Same as V1	3
P4	Aquicludes + *urban*	Aquicludes	Aquicludes	4
Infiltration				*3*
I1	Slopes > 10% in Karstic area	Same as V1	Slopes > 10% in Karstic area + *urban*	2
I2	Slopes < 25% around the coast	Same as V1	Same as V1	3
I3	Rest of the area	Same as V1	Same as V1	4
Karst network development				*2*
K1	Well-developed karst formation	Same as V1	Well-developed karst formation + *urban*	1
K2	Poorly developed karst or aquifers	Same as V1	Same as V1	2
K3	Rest of the area + *urban areas*	Same as V1	Same as V1	3

E (EpiKarst), P (Protective Cover), I (Infiltration Condition), K (Karst network development).
V1: Version one; V2: Version two; V3; Version three.
* The buffering was delineated based on the topography. The measured well with the highest elevation is at 99 m asl, thus that was considered the boundary of the coast in the study areas. Accordingly the maximum distance from the coast to build the buffer was set at 100 m asl.

Index (DI) which is calculated using Eq.(1), where D = Depth to water; R = Recharge; A = Aquifer media, S = Soil media; I = Impact of the Vadose zone; T = Transmissivity; C = Hydraulic conductivity; r = Rating, and w = Weight. Note that the rankings and weights are able to differ from one area to another (Aller et al., 1987; Fijani et al., 2013; Metni et al., 2004; Oroji and Karimi, 2018).

$$DI = D_r D_w + R_r R_w + A_r A_w + S_r S_w + T_r T_w + I_r I_w + C_r C_w \quad (1)$$

Table 3
Water Quality categories with equivalent *DI* and *PF* (or *EI*) ranges.[a]

	Range			
Water Types	TDS (ppm)[b]	DI[c]	Modified EPIK PF (or EI)[d]	Vulnerability
Drinking water	0–500	27–85	32–34	Low
Fresh Water	500–1000	86–106	28–31	
Brackish	1000-5000	107–127	24–27	Moderate
Highly Brackish	5000-15,000	128–148	21–23	
Saline Water	15,000-30,000	149–169	18–20	High
Sea Water	30,000-40,000	170–236	15–17	

[a] Used for assessing the performance of *DRASTIC* and *EPIK* in providing knowledge on contamination distribution in regions known to have unsustainable abstraction leading to seawater intrusion.
[b] Brian, 2012; Costello, 2008
[c] Higher DI values show higher vulnerability and higher salinity levels (Aller et al., 1987; Brian, 2012; SAEFL, 1998; USGS, 2000; Costello, 2008; WHO, 2003).
[d] Lower PF (or EI) values show higher vulnerability and higher salinity levels.

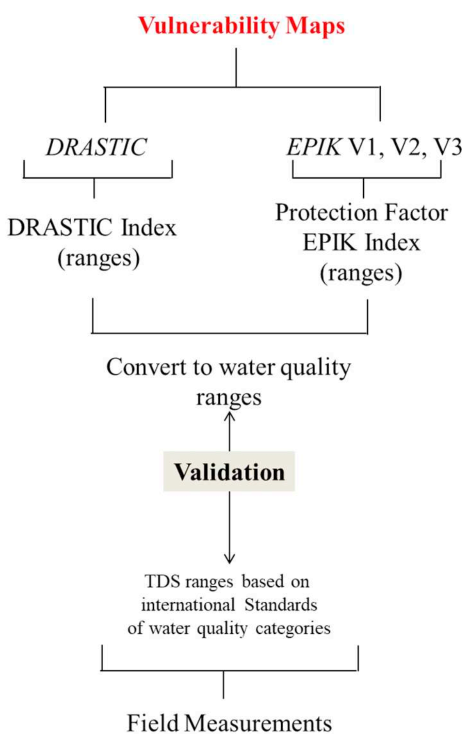

Fig. 4. GVA validation framework.

While *DRASTIC* offers the flexibility in adjusting ratings and weights to fit the specifications of a study area (Kumar et al., 2017; Oroji and Karimi, 2018; Shirazi et al., 2012), it does not differentiate between porous and fractured media nor account for structural geology such as faults or folds (Aller et al., 1987; Fijani et al., 2013; Panagopoulos et al., 2006; Sener and Davraz, 2012). Nevertheless, it has been tested in densely populated areas and in semi-arid zones (Kumar et al., 2015). Its assessment is based on the shallowest aquifer and assumes that contamination is introduced evenly over the study area. The model parameters are often chosen based mostly on a qualitative judgment and its results have mostly not been calibrated or validated by the level of contaminants measured in the field (Kumar et al., 2017; Kura et al., 2015). DRASTIC has been reported as a good approach for tracking seawater intrusion or monitoring the process (Allouche et al., 2017; Kaliraj et al., 2015; Kardan Moghaddam et al., 2017; Zghibi et al., 2016).

EPIK is also an intrinsic GVA model developed by the Swiss Agency for the Environment, Forests and Landscape for karstic environments, spring catchment areas, and well radius of influence (Baalousha, 2016; Hamdan et al., 2016; Kumar et al., 2015; SAEFL, 1998). It has four parameters with weights depending on corresponding impacts and relative importance, with E (Epikarst) and I (Infiltration condition) reported as the most important contributors (SAEFL, 1998). While the K (Karstic Network) is an important parameter (Hamdan et al., 2016), its weight is less than the E parameter (SAEFL, 1998). In the study area, the protective cover (represented by the P parameter) is very thin to non-existent and hence it has the lowest weight. All parameters were divided into sub-categories, each with a specific rating (Fig. 3) (Barrocu et al., 2006; SAEFL, 1998). A *Protection Factor (PF)* or *EPIK Index (EI)* is then calculated using Eq.(2), where E = Epikarst; P = Protective Cover; I = Infiltration Condition; K = Karst Network, and the numbers on the left of the parameters are the suggested weights (SAEFL, 1998).

$$\mathrm{PF\ (or\ EI)} = 3E + 1P + 3I + 2K \qquad (2)$$

Three versions of the *EPIK* model (*EPIKV1, V2, and V3)* were examined to assess its applicability in an urban context (Table 2). In its original form, *EPIK V2* considers the outcrops as the protective cover (P) and thus fails to account for urban areas despite the ability of asphalted areas or concrete structures to create an impermeable surface for the downward percolation of contaminants. To correct for that, *EPIK V1* assumes that urbanization prohibits vertical contamination from infiltration due to its impermeable urban surface thus providing a protective cover resulting in lower vulnerability. This results in urban areas having a lower vulnerable for pollution. On the other hand, *EPIK V3* assumes that urbanization enhances lateral flow due to associated unsustainable abstraction and groundwater overexploitation in highly urbanized zones. The Protection Factor (PF) or EPIK Index (EI) is defined whereby higher scores reflect lower vulnerability areas, and lower scores reflect higher vulnerability areas.

2.3. Validation of Effectiveness of GVA Models

Typically, GVA models do not include a validation step, and when they do, it is usually by qualitative comparison of different GVA results for the same location (Ahmed et al., 2017; Bartzas et al., 2017; Hamdan et al., 2016; Loborec et al., 2015; Michalopoulos and Dimitriou, 2018; Neukum et al., 2008; Ravbar and Goldscheider, 2009). While vulnerability is only a measure of potential or sensitivity to pollution and an area with high vulnerability may not necessarily be polluted at the time of conducting a vulnerability assessment, many studies compared model results with field-measured water quality data (Ahirwar and Shukla, 2018; Ahmed et al., 2017; Allouche et al., 2017; Al-Rawabdeh et al., 2014; Awawdeh and Nawafleh, 2008; Boufekane and Saighi, 2018; Hammouri and El-Naqa, 2008; Haque et al., 2018; Kaliraj et al., 2015; Kardan Moghaddam et al., 2017; Khakhar et al., 2017; Kumar et al., 2016; Kura et al., 2015; Lasagna et al., 2018; Nadiri et al., 2017; Nadjai et al. 2017; Sadat-Noori and Ebrahimi, 2016; Saida et al., 2017; Tiwari et al., 2016; Yang et al., 2017). In this study, an attempt was

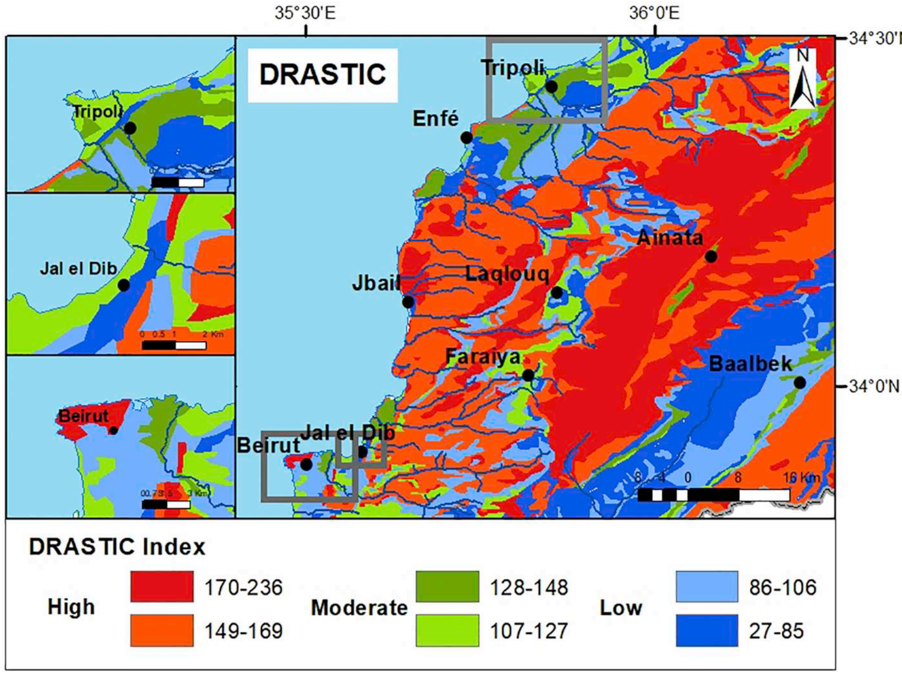

Fig. 5. Groundwater Vulnerbaility based on *DRASTIC Index*.

Table 4
Measured total dissolved solids (WQ_{Field}) and *DRASTIC* ($WQ_{DRASTIC}$) ranges.

WQ_{DRASTIC}	*WQ_{Field}*					
	Drinking water	*Fresh water*	*Brackish*	*Highly brackish*	*Saline water*	*Sea water*
	0–500	*500–1000*	*1000-5000*	*5000-15,000*	*15,000-30,000*	*30,000-40,000*
Beirut						
Drinking water (27–85)	0	0	0	0	0	0
Fresh Water (86–106)	5	43	26	22	6	0
Brackish (107–127)	0	1	2	0	0	0
Highly Brackish (128–148)	2	5	0	0	0	0
Saline Water (149–169)	0	0	0	0	0	0
Sea Water (170–236)	1	2	36	10	4	0
Jal el Dib						
Drinking water (27–85)		2	5	0	0	0
Fresh Water (86–106)	0	1	0	0	0	0
Brackish (107–127)	0	4	14	0	0	0
Highly Brackish (128–148)	0	0	0	0	0	0
Saline Water (149–169)	0	1	0	0	0	0
Sea Water (170–236)	0	0	0	0	0	0
Tripoli						
Drinking water (27–85)	3	1	0	0	0	0
Fresh Water (86–106)	5		0	0	0	0
Brackish (107–127)	18	17	2	0	0	0
Highly Brackish (128–148)	5	4	5	0	0	0
Saline Water (149–169)	0	0	0	0	0	0
Sea Water (170–236)	0	0	0	0	0	0

equally made to assess whether GVA models can provide knowledge on the contamination distribution in coastal aquifers that are experiencing unsustainable groundwater abstraction inducing seawater intrusion. Therefore, an examination was carried out whether areas of high vulnerability should be associated with high groundwater salinity (in the form of TDS as a surrogate) and areas of low vulnerability should be associated with relatively fresh groundwater (assuming uniform spatial abstraction rates), while recognizing that this applies only in regions where saltwater intrusion is the only means of groundwater salinization (Kaliraj et al., 2015; Kardan Moghaddam et al., 2017; Kura et al., 2015;

Table 5
Cumulative percent match for DRASTIC Index score and the defined water quality categories.

ID	*Match (%)*	*± 1 (%)*	*± 2 (%)*	*± 3 (%)*	*± 4/5 (%)*
BEY_DR_TDS	27.3	49.1	71.5	98.2	100
JD_DR_TDS	55.6	77.8	96.3	100	100
TRP_DR_TDS	8.3	55	91.7	100	100

Pilot areas: *BEY* = Beirut; *JD* = Jal el Dib; *TRP* = Tripoli.
DR = *DRASTIC*; *TDS* = Total Dissolved Solids (ppm).
± n indicates the range by which the DI was over- or under- estimating the water quality categories.
n represents the number of categories.

Tabatabaei et al., 2014). Validation is therefore implemented by following a mapping process that links the *DRASTIC Index (DI)* or the *EPIK PF* (or *EPIK Index*) with standardized water quality categories obtained from the water quality measurements. As such, groundwater quality was divided into five categories based on TDS concentrations. Those categories, ranging from freshwater to seawater, were assigned corresponding ranges of *DI* and *PF* (or *EI*) scores based on their qualitative description (Table 3). If *DRASTIC* and *EPIK* can provide knowledge on contamination distribution, then low vulnerability zones would be less likely to have deteriorated groundwater quality. In contrast, zones categorized as high vulnerability would be more likely to have deteriorated groundwater quality as a result of saltwater intrusion. Thus, the groundwater that qualifies to be of the "Drinking Water" category is expected to be more commonly encountered in areas with low vulnerability zones and the "Sea Water" category is more probable in areas falling within high vulnerability zones. Evidently this assessment is not meant to evaluate *DRASTIC* and *EPIK's* ability to simulate groundwater quality, but rather to check if water quality distributes itself following trends predicted by vulnerability maps. This assumption is evaluated under the condition that the entire study area is experiencing unsustainable abstraction practices causing seawater intrusion. The categories of *DI* and *PF* (or *EI*) were divided equally between the low and high vulnerability thresholds, where higher *DI* values show higher vulnerability and more deteriorated groundwater quality, and lower *PF* (or *EI*) values show higher vulnerability and more deteriorated water quality. Fig. 4 summarizes the adopted approach towards linking the vulnerability assessment of the aquifer with the status of the groundwater quality.

3. Results and discussion

3.1. *DRASTIC*

Fig. 5 presents the groundwater vulnerbaility based on the *DRASTIC Index* values. It is evident that karstification regions in the high land, marked with red, have a high vulnerability whereas the plains with soil cover and recent less-permeable outcrops are designated with blue to green indicating lower vulnerability. The coast varies from low to moderate to high vulnerability in the south, north, and midland areas, respectively. The vulnerability is based on 1:200,000 geologic map, which highlights the focus of this methodology on the outcropping lithology and not necessarily the underlying aquifers (Table SP-1). The overall map also shows how the anthropogenic factor is left uncounted for when analyzing the vulnerability of the system.

The analysis for the percent match between water quality categories forecasted by *DRASTIC* and those obtained from field groundwater quality analysis in the three pilot areas was conducted to verify the extent of the match between the ranges based on field measured data and the ranges predicted by *DRASTIC* (Table 4). Ideally, elements would fall along the diagonals. Off-diagonal elements can provide an idea on the tendency of *DRASTIC* to over-estimate or under-estimate groundwater quality vulnerability. Values in the upper triangle indicate over-estimation, while the lower triangle values reflect under-estimation.

DRASTIC's ability to correctly predict the extent of pollution from saltwater intrusion ranged from 8.3% (5 wells out of 60) in Tripoli to 55.6% (15 wells out of 27) in Jal el Dib, with Beirut in the middle at 27.3% (47 wells out of 165). Furthermore, *DRASTIC*'s ability to predict within ± 1 water quality category ranged from 49.1% in Beirut to 77.8% in Jal el Dib with Tripoli at 55% (Table 5). While the performance of *DRASTIC* in Jal el Dib was good, in Beirut was poor, where nearly one third (28.5%) of the water quality predictions were off by 3 or more water quality categories. In order to ensure that these diversions within categories are not based on errors in measuring the water quality, an error estimation of ± 3% (Wagner et al., 2006) of water quality readings was added on TDS measurements, and the number of points which crossed categories due to this error were counted. No significant changes were observed. Table 5 summarizes the crosscheck results for *DRASTIC* for the three pilot areas using TDS as a proxy indicator. The Match column shows when *DRASTIC Index* results which perfectly matched with the water quality categories defines by the field measurements. The remaining columns highlight the over and under estimation issues of the model in the three study sites.

3.2. *EPIK*

A comparison between the three versions of *EPIK* along the coastline covering the three cities is shown in Fig. 6 and Table SP-2. The comparison shows a similarity between the three approaches except in highly urbanized regions along the coast. *EPIK V1* included urbanization as a surface of protection, which may be true in surface-induced-contamination, but not necessarily so for many coastal cities in developing countries, where urbanization is adding on the vulnerability because of increased abstraction inducing seawater intrusion laterally. While *EPIK V1* showed that the coastline is mainly of moderate vulnerability, in *EPIK V2,* urbanization is not considered, and the vulnerability is taken solely based on the geological outcrops. In contrast, *EPIK V3* assigns higher vulnerability to coastal urban areas to emphasize the anthropogenic impact of groundwater extraction resulting in a noticeable increase in vulnerability along the coastal areas under *EPIK V3*.

A similar validation procedure for the three cities was tested using the three versions *EPIK V1, EPIK V2,* and *EPIK V3* with the results presented in Tables 6, 7, and 8, respectively. Once again, values in the diagonal cells indicate the level of match between the water quality classes and the classes produced based on the *PF* (or *EI*) results of the *EPIK* vulnerability assessment. In *EPIK V1,* where urbanization means low impact zone, measurements in Beirut correlated by about 23% with *PF* (or *EI*) values, whereas in Tripoli and Jal el Dib the correlation reached only 11% and 78%, respectively. In *EPIK V2,* where there is no urbanization factor, over 70% correlation was observed for Jal el Dib measurements; whereas, Beirut and Tripoli had similar correlation values as the previous version, 24% and 11%, respectively. In *EPIK V3,* where urbanization is a high impact zone, there is no correlation in

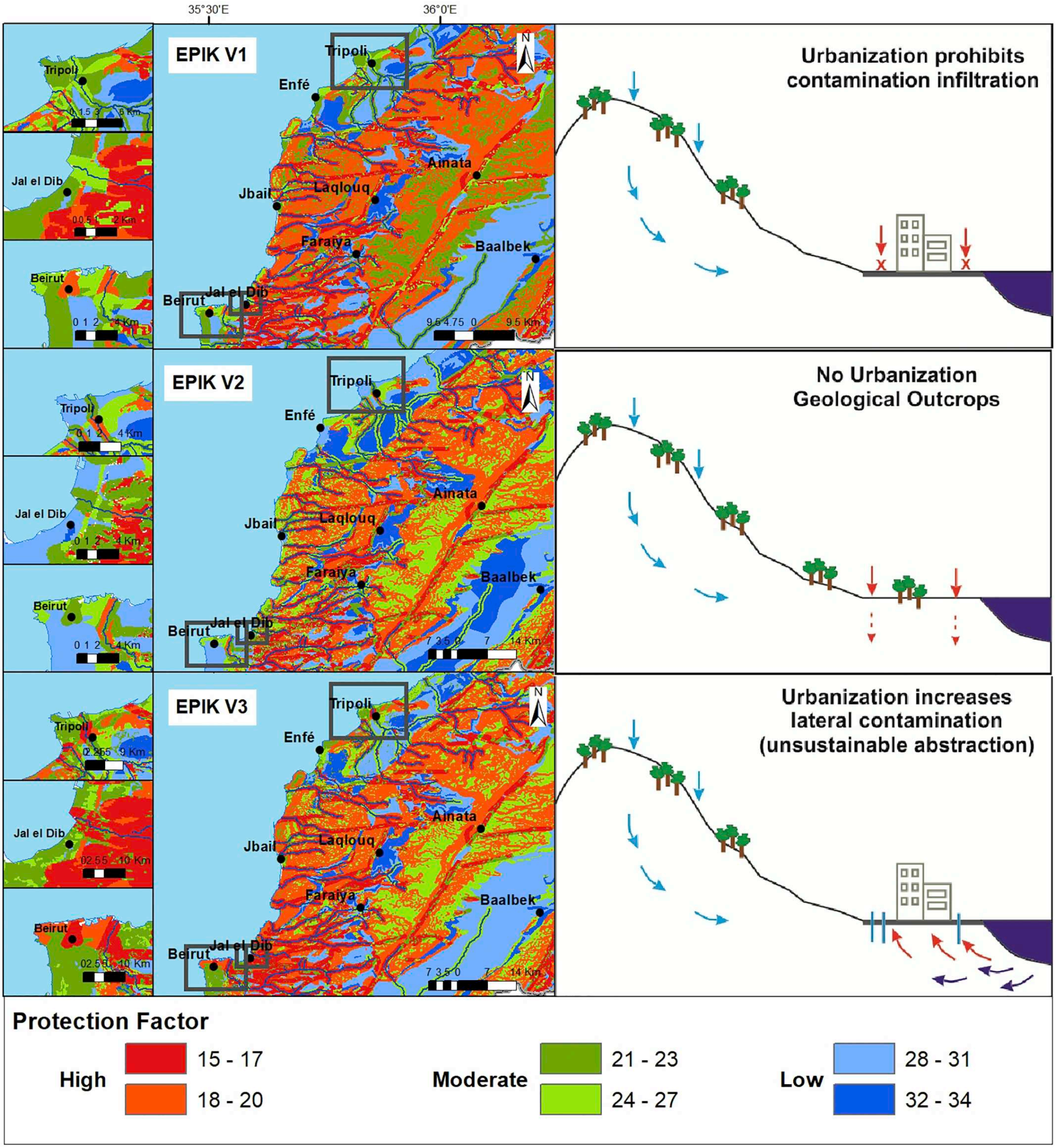

Fig. 6. Right: Groundwater vulnerability based on the 3 versions of *EPIK* Protection Factors or EPIK Indices.
Center: *EPIK* results at the regional scale for the three versions.
Left: *EPIK* results for Tripoli, Jal el Dib, and Beirut using the three versions of *EPIK*.

Table 6
Measured Total Dissolved Solids (WQ_{Field}) and *EPIK V1* ($WQ_{EPIK\ V1}$).

$WQ_{EPIK\ V1}$	*WQ_{Field}*					
	Drinking water	*Fresh water*	*Brackish water*	*Highly brackish*	*Saline water*	*Sea water*
	0–500	*500–1000*	*1000–5000*	*5000–15,000*	*15,000–30,000*	*30,000–40,000*
Beirut						
Drinking water (32–34)	0	0	0	0	0	0
Fresh Water (28–31)	0	8	6	0	0	0
Brackish (24–27)	2	12	24	18	6	0
Highly Brackish (21 – 23)	4	11	21	4	1	0
Saline Water (18–20)	2	20	13	10	3	0
Sea Water (15–17)	0	0	0	0	0	0
Jal el Dib						
Drinking water (32–34)		0	0	0	0	0
Fresh Water (28–31)	0	3	1	0	0	0
Brackish (24–27)	0	5	18	0	0	0
Highly Brackish (21–23)	0	0	0	0	0	0
Saline Water (18–20)	0	0	0	0	0	0
Sea Water (15–17)	0	0	0	0	0	0
Tripoli						
Drinking water (32–34)	0	0	0	0	0	0
Fresh Water (28–31)	1	0	0	0	0	0
Brackish (24–27)	24	22	7	0	0	0
Highly Brackish (21–23)	6	0	0	0	0	0
Saline Water (18–20)	0	0	0	0	0	0
Sea Water (15–17)	0	0	0	0	0	0

Table 7
Measured total dissolved solids (WQ_{Field}) and *EPIK V2* ($WQ_{EPIK\ V2}$) ranges.

$WQ_{EPIK\ V2}$	*WQ_{Field}*					
	Drinking water	*Fresh water*	*Brackish water*	*Highly Brackish*	*Saline water*	*Sea water*
	1–500	*500–1000*	*1000–5000*	*5000–15,000*	*15,000–30,000*	*30,000–40,000*
Beirut						
Drinking water (32–34)	0	0	0	0	0	0
Fresh Water (28–31)	0	8	6	0	0	0
Brackish (24–27)	2	14	25	19	7	0
Highly Brackish (21–23)	4	12	23	5	1	0
Saline Water (18–20)	2	17	10	8	2	0
Sea Water (15–17)	0	0	0	0	0	0
Jal el Dib						
Drinking water (32–34)	0	0	0	0	0	0
Fresh Water (28–31)	0	3	1	0	0	0
Brackish (24–27)	0	5	18	0	0	0
Highly Brackish (21–23)	0	0	0	0	0	0
Saline Water (18–20)	0	0	0	0	0	0
Sea Water (15–17)	0	0	0	0	0	0
Tripoli						
Drinking water (32–34)	0	0	0	0	0	0
Fresh Water (28–31)	1	0	0	0	0	0
Brackish (24–27)	25	22	7	0	0	0
Highly Brackish (21–23)	5	0	0	0	0	0
Saline Water (18–20)	0	0	0	0	0	0
Sea Water (15–17)	0	0	0	0	0	0

water quality measurements and vulnerability assessment in Tripoli, whereas in Beirut and Jal el Dib, the match is around 10% and 11%, respectively (Tables 6–8).

A summary of the adequacy of the three versions across the three cities is presented in Tables 9. *EPIK V3* (with urbanization causing a larger impact that should produce higher vulnerabilities) did not prove to generate an improvement when compared to the other two versions, indicating the inability of *EPIK* to account for urbanization and predict the variability of saltwater intrusion in coastal urban areas. This is also an indication that while *EPIK* can reflect on the physical characteristics

Table 8
Measured Total Dissolved Solids (WQ_{Field}) and *EPIK V3* ($WQ_{EPIK\ V3}$) ranges.

$WQ_{EPIK\ V3}$	WQ_{Field}					
	Drinking water	*Fresh water*	*Brackish water*	*Highly Brackish*	*Saline Water*	*Sea water*
	1–500	*500–1000*	*1000–5000*	*5000–15,000*	*15,000-30,000*	*30,000–40,000*
Beirut						
Drinking water (32–34)	0	0	0	0	0	0
Fresh Water (28–31)	0	0	0	0	0	0
Brackish (24–27)	0	0	0	0	0	0
Highly Brackish (21–23)	2	18	29	17	6	0
Saline Water (18–20)	4	10	22	5	1	0
Sea Water (15–17)	2	23	13	10	3	0
Jal el Dib						
Drinking water (32–34)	0	0	0	0	0	0
Fresh Water (28–31)	0	1	0	0	0	0
Brackish (24–27)	0	1	2	0	0	0
Highly Brackish (21–23)	0	6	17	0	0	0
Saline Water (18–20)	0	0	0	0	0	0
Sea Water (15–17)	0	0	0	0	0	0
Tripoli						
Drinking water (32–34)	0	0	0	0	0	0
Fresh Water (28–31)	1	0	0	0	0	0
Brackish (24–27)	4	8	0	0	0	0
Highly Brackish (21–23)	22	13	7	0	0	0
Saline Water (18–20)	2	0	0	0	0	0
Sea Water (15–17)	2	1	0	0	0	0

Table 9
Cumulative Percent of match for the three *EPIK* versions scores and defined water quality categories.

ID	*Match (%)*	*± 1 (%)*	*± 2 (%)*	*± 3 (%)*	*± 4/5 (%)*
EPIK V1					
BEY_EP1_TDS	23.6	64.8	84.2	98.8	100
JD_EP1_TDS	77.8	100	100	100	100
TRP_EP1_TDS	11.7	50	90	100	100
EPIK V2					
BEY_EP2_TDS	24.2	67.2	86	98.7	100
JD_EP2_TDS	77.8	100	100	100	100
TRP_EP2_TDS	11.7	50	91.7	100	100
EPIK V3					
BEY_EP3_TDS	10.9	37	67.3	82.5	100
JD_EP3_TDS	11.1	77.8	100	100	100
TRP_EP3_TDS	0	26.7	55	91.7	100

BEY = Beirut; *JD* = Jal el Dib; *TRP* = Tripoli.
EPIK V1 (EP1): urbanization low impact; *EPIK V2 (EP2)*: no urbanization; *EPIK V3 (EP3)*: urban areas high vulnerability.
TDS = Total Dissolved Solids (ppm).
± n indicates the range by which the score was over or under estimating the water quality categories. n represents the number of categories.

of an aquifer, it can't account for the anthropogenic impacts.

3.3. *EPIK versus DRASTIC for water quality assessment*

EPIK and *DRASTIC* are vulnerability assessment models and were not designed to predict water quality measurements taken from the field. However, since this comparison is a practice that is common in some of the existing literature (Elewa et al., 2013; Selmi, 2013; Jamrah et al., 2008; Chachadi and Lobo-Ferreira, 2005; Chachadi and Lobo-Ferreira, 2001), this study targeted a cross-validation to test the validity of this practice. Overall, *DRASTIC* and *EPIK* performed poorly indicating that utilizing vulnerability assessment models for inferring patterns of water quality affected by anthropogenic stresses like over-abstraction is not recommended. The *EPIK V3* (urbanization as higher vulnerability) exhibited the weakest performance, with the other two versions performing relatively better than *DRASTIC* (Tables 5 and 9), with *EPIK V2* (no urbanization) performing the best among the GVA models. Nevertheless, both models use physical characteristics which correlated well with the geology of the study area (Fig. 7).

4. Concluding remarks

DRASTIC and *EPIK* were tested for their ability to evaluate the vulnerability of coastal aquifers under anthropogenic interventions in the form of overexploitation of groundwater to meet chronic water shortages associated with population growth, increased urbanization and development, as well as potential climate change impacts. An attempt was made to examine the ability of these models to assess groundwater quality distribution in coastal urban karstic areas experiencing seawater intrusion. While the vulnerability mapping can be helpful for water and land use policy planning for protection before the occurrence of a polluting event, the model simulations exhibited weak correlation with field measurements of saltwater intrusion induced by anthropogenic activities emphasizing their limited abilities in defining quality conditions / patterns after the occurrence of a polluting event.

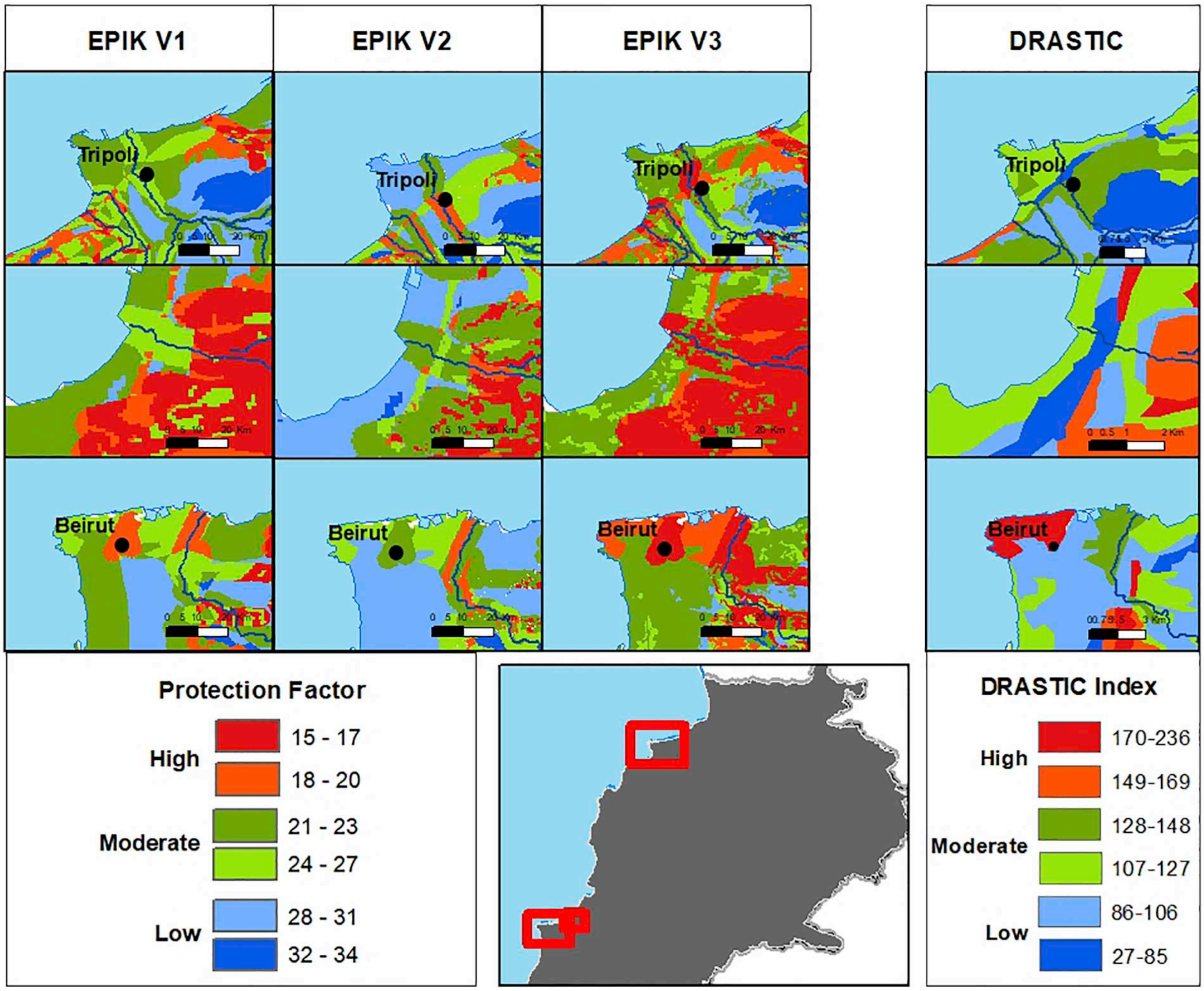

Fig. 7. Comparison between EPIK and DRASTIC.

Acknowledgements

This study is part of a program on climate change and seawater intrusion along the Eastern Mediterranean funded by the International Development Research Center (IDRC) of Canada at the American University of Beirut Grant No. 106706-001. Special thanks are extended to Dr. Charlotte Macalister at IDRC for her support and feedback in implementing this program.

Appendix A. Supplementary data

Supplementary data to this article can be found online at https://doi.org/10.1016/j.eiar.2018.10.003.

References

Ahirwar, S., Shukla, J.P., 2018. Assessment of groundwater vulnerability in upper betwa river watershed using GIS based DRASTIC model. J. Geol. Soc. India 91 (3), 334–340.
Ahmadian, S., 2013. Geostatistical based modelling of variations of groundwater quality during 2006 to 2009 (in Tehran-Karaj Plain). J. Basic Appl. Sci. Res. 3 (2s), 264–272.
Ahmed, I., Nazzal, Y., Zaidi, F., 2017. Groundwater pollution risk mapping using modified DRASTIC model in parts of Hail region of Saudi Arabia. Environ. Eng. Res. 23 (1), 84–91.
Alam, F., Umar, R., Ahmed, S., Dar, F.A., 2014. A new model (DRASTIC-LU) for evaluating groundwater vulnerability in parts of central Ganga Plain, India. Arab. J. Geosci. 7 (3), 927–937.
Aller, L., Lehr, J.H., Petty, R., 1987. DRASTIC: A Standardized System to Evaluate Ground Water Pollution Potential Using Hydrogeologic Settings. National Water Well Association, Worthington, Ohio.
Allouche, N., Maanan, M., Gontara, M., Rollo, N., Jmal, I., Bouri, S., 2017. A global risk approach to assessing groundwater vulnerability. Environ. Model Softw. 88, 168–182.
Al-Rawabdeh, A., Al-Ansari, N., Al-Taani, A., Al-Khateeb, F., Knutsson, S., 2014. Modeling the risk of groundwater contamination using modified DRASTIC and GIS in Amman-Zerqa Basin, Jordan. Open Eng. 4 (3), 264–280.
APHA/AWWA/WEF, 2012. American Public Health Association, American Water Works Association, and Water Environment Federation. Standard Methods of Water and Wastewater, 22nd ed. American Public Health Association.
Awad, M.M., Darwich, T., 2009. Evaluating sea water quality in the coastal zone of North Lebanon using Telemac-2D. Lebanese Sci. J. 10 (1), 35–43.
Awawdeh, M., Nawafleh, A., 2008. A GIS-based EPIK model for assessing aquifer vulnerability in Irbid Governorate, North Jordan. Jordan J. Civil Eng. 2 (3), 267–278.
Baalousha, H.M., 2016. Groundwater vulnerability mapping of Qatar aquifers. J. Afr. Earth Sci. 124, 75–93.
Barrocu, G., Muzzu, M., Uras, G., 2006. Hydrogeology and vulnerability map (EPIK method) of the “Supramonte” karstic system, north-central Sardinia. Environ. Geol. 51 (5), 701–706.
Bartzas, G., Zaharaki, D., Doula, M., Komnitsas, K., 2017. Evaluation of groundwater vulnerability in a Greek island using GIS-based models. Desalin. Water Treat. 67, 61–73.
Boufekane, A., Saighi, O., 2018. Application of Groundwater Vulnerability Overlay and Index Methods to the Jijel Plain Area (Algeria). Groundwater 56 (1), 143–156.
Brian, O., 2012. Water Quality-your private well: what do the results mean. Wilkes University.
Center, Meteorological, 1977. Atlas Climatique Du Liban (V 1A). Beirut. Directorate general of the civil aviation.
Central Administration of Statistics, 2009. Population characteristics in 2009 – Final Report. UNICEF.
Chachadi, A.G., Lobo-Ferreira, J.P., 2001. Sea water intrusion Vulnerability mapping of aquifers using the GALDIT method. In: *Coastin: a Coastal Policy Research Newsletter.* DG XII. vol. 4. TERI and European Commission, pp. 7–9.
Chachadi, A.G., Lobo-Ferreira, J.-P., 2005. Assessing Aquifer Vulnerability to seawater intrusion using GALDIT method: Part 2- GALDIT Indicators Description. *The fourth Inter-Celtic Colloquium on Hydrology and Management of Water Resources*. Guimaraes, Portugal.

Chachadi, A.G., Lobo-Ferreira, J.P., Noronha, L., 2002. Assessing the impact of sea-level rise on salt water intrusion in coastal aquifers using GALDIT model. In: *Coastin: a Coastal Policy Research Newsletter*. DG XII. 7. TERI and European Commission, pp. 27–32.

Chang, N.-B., 2010. Effects of Urbanization on Groundwater : An Engineering Case-based Approach for Sustainable Development. American Society of Civil Engineers, Reston, Virginia.

Colins, J., Sashikkumar, M.C., Anas, P.A., Kirubakaran, M., 2016. GIS-based assessment of aquifer vulnerability using DRASTIC Model: A case study on Kodaganar basin. Earth Sci. Res. J. 20 (1), 1–8.

Costello, M., 2008. Salt Water Definition Review (Draft RWF Task Group). National Sanitation Foundation (NSF) Standards, Water Quality Assosiation.

De Filippis, G., Foglia, L., Giudici, M., Mehl, S., Margiotta, S., Negri, S.L., 2016. Seawater intrusion in karstic, coastal aquifers: Current challenges and future scenarios in the Taranto area (southern Italy). Sci. Total Environ. 573, 1340–1351.

Doerfliger, N., 1996. Advances in karst groundwater protection strategy using artificial tracer test analysis on a multiattribute vulnerability mapping (EPIK method). PhD Dissertation. University of Neuchatel, Neuchatel, Switzerland.

Doerfliger, N., Jeannin, P.-Y., Zwahlen, F., 1999. Water vulnerability assessment in karst environments: a new method of defining protection areas using a multi-attribute approach and GIS tools (EPIK method). Environ. Geol. 39 (2), 165–176.

Dubertret, L., 1955. Carte geologique du Liban 1: 200 000, L'Association des Amis de Ibrahim Abd El Al.

Edgell, H.S., 1997. Karst and hydrogeology of Lebanon. Carbonates Evaporites 12 (2), 220.

ELARD, 2015. Provision of assessing the national groundwater resources through data collection and field assessment campaign of groundwater resources across Lebanon: a case study Nabaa AlAssal. Pari V - Vulnerability assessment using COP + K. (Unpublished work).

Elewa, H.H., Shohaib, R.E., Qaddah, A.A., Nousir, A.M., 2013. Determining groundwater protection zones for the Quaternary aquifer of northeastern Nile Delta using GIS-based vulnerbaility mapping. Environ. Earth Sci. 68, 313–331.

El-Fadel, M., Maroun, R., Semerjian, L., Harajli, H., 2003. A health-based socio-economic assessment of drinking water quality: the case of Lebanon. Manag. Environ. Qual. 14 (3), 353–368.

El-Fadel, M., Rachid, G., Alameddine, I., Abu, Najm M., 2014a. Saltwater Intrusion in karst aquifers along the Eastern Mediterranean. 23rd Salt Water Intrusion Meeting - SWIM23. June 16–20, 2014, Husum, Germany.

El-Fadel, M., Tomaszkiewicz, M., Adra, Y., Sadek, S., Abou Najm, M., 2014b. GIS-Based Assessment for the Development of a Groundwater Quality Index Towards Sustainable Aquifer Management. Water Resour. Manag. 28 (11), 3471–3487.

Fetter, C.W., 2001. Applied hydrogeology. Upper Saddle River, Prentice Hall, New Jersey.

Fijani, E., Nadiri, A.A., Asghari Moghaddam, A., Tsai, F.T.C., Dixon, B., 2013. Optimization of DRASTIC method by supervised committee machine artificial intelligence to assess groundwater vulnerability for Maragheh–Bonab plain aquifer, Iran. J. Hydrol. 503, 89–100.

Focazio, M.J., 2002. Assessing Ground-Water Vulnerability to Contamination: Providing Scientifically Defensible Information for Decision Makers. vol. 1224 US Dept. of the Interior, US Geological Survey.

Ghazavi, R., Ebrahimi, Z., 2015. Assessing groundwater vulnerability to contamination in an arid environment using DRASTIC and GOD models. Int. J. Environ. Sci. Technol. 12 (9), 2909–2918.

Gogu, R.C., Dassargues, A., 2000a. Current trends and future challenges in groundwater vulnerability assessment using overlay and index methods. Environ. Geol. 39 (6), 549–559.

Gogu, R.C., Dassargues, A., 2000b. Sensitivity analysis for the EPIK method of vulnerability assessment in a small karstic aquifer, southern Belgium. Hydrogeol. J. 8 (3), 337–345.

Gogu, R.C., Hallet, V., Dassargues, A., 2003. Comparison of aquifer vulnerability assessment techniques. Application to the Neblon river basin (Begium). Environ. Geol. 44, 881–892.

Goldscheider, N., 2005. Karst groundwater vulnerbaility mapping: application of a new method in the Swabian Alb, Germany. Hydrogeol. J. 13 (4), 555–564.

Hamdan, I., Margane, A., Ptak, T., Wiegand, B., Sauter, M., 2016. Groundwater vulnerability assessment for the karst aquifer of Tanour and Rasoun springs catchment area (NW-Jordan) using COP and EPIK intrinsic methods. Environ. Earth Sci. 75 (23), 1474.

Hammouri, N., El-Naqa, A., 2008. GIS based hydrogeological vulnerability mapping of groundwater resources in Jerash area-Jordan. Geofis. Int. 47 (2), 85–97.

Hao, J., Zhang, Y., Jia, Y., Wang, H., Niu, C., Gan, Y., Gong, Y., 2017. Assessing groundwater vulnerability and its inconsistency with groundwater quality, based on a modified DRASTIC model: a case study in Chaoyang District of Beijing City. Arab. J. Geosci. 10 (6), 144.

Haque, E., Reza, S., Ahmed, R., 2018. Assessing the vulnerability of groundwater due to open pit coal mining using DRASTIC model: a case study of Phulbari Coal Mine, Bangladesh. Geosci. J. 22 (2), 359–371.

Howard, K.W.F., 2002. In: Howard, K.F., Israfilov, R. (Eds.), Urban Groundwater Issues—An Introduction. Current Problems of Hydrogeology in Urban Areas, Urban Agglomerates and Industrial Centres. 8. Springer, Netherlands, pp. 1–15.

IPCC, Tignor, M.B., Allen, S.K., Boschung, J., Nauels, A., YuXia, V. Bex, Midgley, P.M., 2013. In: Stocker, T.F., Qin, D., Plattner, G.-K. (Eds.), Climate Change (IPCC 5): The physical science basis. Contribution of Working Group I to the Fifth Assessment Report of the IPCC. vol. 1535 C. U. Press. Cambrige, UK and New York, US.

Jamrah, A., Al-Futaisi, A., Rajmohan, N., Al-Yarubi, S., 2008. Assessment of groundwater vulnerability in the coastal region of Oman using DRASTIC index method in GIS environment. Environ. Monit. Assess. 147 (1–3), 125–138.

Jarray, H., Zammouri, M., Ouessar, M., Zerrim, A., Yahyaoui, H., 2017. GIS based DRASTIC model for groundwater vulnerability assessment: Case study of the shallow mio-plio-quaternary aquifer (Southeastern Tunisia). Water Resources 44 (4), 595–603.

Kaliraj, S., Chandrasekar, N., Peter, T.S., Selvakumar, S., Magesh, N.S., 2015. Mapping of coastal aquifer vulnerable zone in the south west coast of Kanyakumari, South India, using GIS-based DRASTIC model. Environ. Monit. Assess. 187 (1), 4073.

Kallioras, A., Pliakas, F., Skias, S., Gkiougkis, I., 2011. Groundwater vulnerability assessment at SW Rhodope aquifer system in NE Greece. In: Lambrakis, N., Stournaras, G., Katsanou, K. (Eds.), Advances in the Research of Aquiatic Environment. Springer, New York.

Kardan Moghaddam, H., Jafari, F., Javadi, S., 2017. Vulnerability evaluation of a coastal aquifer via GALDIT model and comparison with DRASTIC index using quality parameters. Hydrol. Sci. J. 62 (1), 137–146.

Kazakis, N., Oikonomidis, D., Voudouris, K.S., 2015. Groundwater vulnerability and pollution risk assessment with disparate models in karstic, porous, and fissured rock aquifers using remote sensing techniques and GIS in Anthemountas basin, Greece. Environ. Earth Sci. 74 (7), 6199–6209.

Khakhar, M., Ruparelia, J.P., Vyas, A., 2017. Assessing groundwater vulnerability using GIS-based DRASTIC model for Ahmedabad district, India. Environ. Earth Sci. 76 (12), 440.

Khan, M.M.A., Umar, R., Lateh, H., 2010. Assessment of aquifer vulnerability in parts of Indo Gangetic plain, India. Int. J. Phys. Sci. 5 (11), 1711–1720.

Kumar, S., Thirumalaivasan, D., Radhakrishnan, N., 2014. GIS based assessment of groundwater vulnerability using drastic model. Arab. J. Sci. Eng. 39 (1), 207–216.

Kumar, P., Bansod, B.K.S., Debnath, S.K., Thakur, P.K., Ghanshyam, C., 2015. Index-based groundwater vulnerability mapping models using hydrogeological settings: A critical evaluation. Environ. Impact Assess. Rev. 51, 38–49.

Kumar, P., Thakur, P.K., Bansod, B.K., Debnath, S.K., 2016. Assessment of the effectiveness of DRASTIC in predicting the vulnerability of groundwater to contamination: a case study from Fatehgarh Sahib district in Punjab, India. Environ. Earth sci. 75 (10), 879.

Kumar, P., Thakur, P.K., Bansod, B.K., Debnath, S.K., 2017. Multi-criteria evaluation of hydro-geological and anthropogenic parameters for the groundwater vulnerability assessment. Environ. Monit. Assess. 189 (11), 564.

Kumari, S., Jha, R., Singh, V., Baier, K., Sinha, M.K., 2016. Groundwater Vulnerability Assessment using SINTACS Model and GIS in Raipur and Naya Raipur, Chhattisgarh, India. Ind. J. Sci. Technol. 9 (41).

Kura, N.U., Ramli, M.F., Ibrahim, S., Sulaiman, W.N.A., Aris, A.Z., Tanko, A.I., Zaudi, M.A., 2015. Assessment of groundwater vulnerability to anthropogenic pollution and seawater intrusion in a small tropical island using index-based methods. Environ. Sci. Pollut. Res. 22 (2), 1512–1533.

Lasagna, M., De Luca, D.A., Franchino, E., 2018. Intrinsic groundwater vulnerability assessment: issues, comparison of different methodologies and correlation with nitrate concentrations in NW Italy. Environ. Earth Sci. 77 (7), 277.

Loáiciga, H.A., Pingel, T.J., Garcia, E.S., 2012. Sea Water Intrusion by Sea-Level Rise: Scenarios for the 21st Century. Ground Water 50 (1), 37–47.

Lobo-Ferreira, J.P., Chachadi, A.G., Diamantino, C., Henriques, M.J., 2007. Assessing aquifer vulnerability to seawater intrusion using the GALDIT method. Part 1-application to the Portuguese monte gordo aquifer. IAHS-AISH publication, pp. 161–171.

Loborec, J., Kapelj, S., Dogančić, D., Siročić, A.P., 2015. Assessment of groundwater vulnerability in Croatian karstic aquifer in Jadro and Žrnovnica springs catchment area. In: Hydrogeological and Environmental Investigations in Karst Systems. Springer, Berlin, Heidelberg, pp. 397–405.

Magiera, P., 2000. Methoden zur Abschatzung der Verschmutzungsempfind-lichkeit des Grundwassers (Methods for Assessment of Pollution Groundwater Vulnerability). Grundwasser 5 (3), 103–114.

Mahmoudzadeh, E., Rezaian, S., Ahmadi, A., 2013. Assessment of Meymeh Plain Aquifer Vulnerability in Esfahan Using Comparative Method AVI, GODS, DRASTIC.

Marin, A., Andreo, B., Mudarra, M., 2010a. Importance of evaluating karst features in contamination vulnerability and groundwater protection assessment of carbonate aquifers. the case study of alta cadena (southern spain). Zeitschrift Fur Geomorphologie 54, 179–194.

Marin, A.I., Dörfliger, N., Andreo, B., 2010b. In: Andreo, B., Carrasco, F., Durán, J.J., LaMoreaux, J.W. (Eds.), Comparative Application of Two Methods (COP and PaPRIKa) for Groundwater Vulnerability Mapping in the Lez Karst System (Montpellier, South France). Advances in Research in Karst Media Springer, Berlin Heidelberg, pp. 329–334.

Metni, M., El-Fadel, M., Sadek, S., Kayal, R., El-Khoury, D.L., 2004. Groundwater Resources in Lebanon: A Vulnerability Assessment. Water Resour. Manag. 20 (4), 475–491.

Michalopoulos, D., Dimitriou, E., 2018. Assessment of pollution risk mapping methods in an Eastern Mediterranean catchment. J. Ecol. Eng. 19 (1).

Milnes, E., 2011. Process-based groundwater salinisation risk assessment methodology: Application to the Akrotiri Aquifer (Southern Cyprus). J. Hydrol. 399, 29–47.

Nadiri, A.A., Gharekhani, M., Khatibi, R., Moghaddam, A.A., 2017. Assessment of groundwater vulnerability using supervised committee to combine fuzzy logic models. Environ. Sci. Pollut. Res. 24 (9), 8562–8577.

Najib, S., Grozavu, A., Mehdi, K., Breaban, I.G., Guessir, H., Boutayeb, K., 2012. Application of the method galdit for the cartography of groundwaters vulnerability: aquifer of Chaouia coast (Morocco). vol. 58(2). Analele Stiintifice ale Universitatii Al. I. Cuza din Iasi, Serie Noua. Geografie, pp. 77.

Neh, A.V., Ako, A.A., Ayuk II, A.R., Hosono, T., 2015. DRASTIC-GIS model for assessing vulnerability to pollution of the phreatic aquiferous formations in Douala–Cameroon. J. Afr. Earth Sci. 102, 180–190.

Neukum, C., Hötzl, H., Himmelsbach, T., 2008. Validation of vulnerability mapping

methods by field investigations and numerical modelling. Hydrogeol. J. 16 (4), 641–658.
Oroji, B., Karimi, Z.F., 2018. Application of DRASTIC model and GIS for evaluation of aquifer vulnerability: case study of Asadabad, Hamadan (western Iran). Geosci. J. 1–13.
Panagopoulos, G.P., Antonakos, A.K., Lambrakls, N.J., 2006. Optimization of the DRASTIC method for groundwater vulnerability assessment via the use of simple statistical methods and GIS. Hydrogeol. J. 14, 894–911.
Pera, S., Valcarce, R.M., 2009. Groundwater vulnerability assessment in La Habana city area, Cuba. In: Applied Research Partnership with Developing and Transition Countries. Institute of Earth Sciences, Canobbio; Politecnico Jose Antonio Echeveria, La Habana.
Polemio, M., Casarano, D., Linoni, P.P., 2009. Karstic aquifer vulnerability assessment methods and results at a test site (Apulia, southern Italy). Nat. Hazards Earth Syst. Sci. 9, 1461–1470.
Rangel-Medina, M., Rogelio Monreal, S., Mariano Morales, M., Gurrola, Jose Castillo, 2004. Estimation of vulnerbaility to saline intrusion. Geofis. Int. 43 (4), 611–621.
Ranjan, P., Kazama, S., Sawamoto, M., 2006. Effects of climate change on coastal fresh groundwater resources. Glob. Environ. Chang. 16 (4), 388–399.
Ravbar, N., Goldscheider, N., 2009. Comparative application of four methods of groundwater vulnerability mapping in a Slovene karst catchment. Hydrogeol. J. 17 (3), 725–733.
Sadat-Noori, M., Ebrahimi, K., 2016. Groundwater vulnerability assessment in agricultural areas using a modified DRASTIC model. Environ. Monit. Assess. 188 (1), 19.
SAEFL (Swiss Agency for Environment, Forests and Landscape), 1998. Practical Guide: Groundwater Vulnerability Mapping in Karstic Regions (EPIK). Application to Groundwater Protection Zones.
Saidi, S., Bouri, S., Hassine, S., Ben Dhia, H., 2014. Comparison of three applied methods of groundwater vulnerability mapping: application to the coastal aquifer of Chebba–Mellouleche (Tunisia). Desalination and Water Treat. 52 (10-12), 2120–2130.
Salemi, E., Colombani, N., Aschonitis, V., Mastrocicco, M., 2011. Assessment of specific vulnerbaility to nitrates using LOS indices in the Ferrara Province, Italy. In: Lambrakis, N., Stournaras, G., Katsanou, K. (Eds.), Advances in the Research of Aquiatic Environment. Springer, New York.
Selmi, A., 2013. Water management and modeling of a coastal aquifer case study (Gaza strip). Doctoral dissertation, Thesis. Faculty of Mathematics, Physics and Natural Sciences, Italy.
Sener, E., Davraz, A., 2012. Assessment of groundwater vulnerability based on a modified DRASTIC model, GIS and an analytic hierarchy process (AHP) method: the case of Egirdir Lake basin (Isparta, Turkey). Hydrogeol. J. 21 (3), 701–714.
Shirazi, S.M., Imran, H.M., Akib, S., 2012. GIS-based DRASTIC method for groundwater vulnerbaility assessment: A review. J. Risk Res. 15 (8), 991–1011.
Sinha, M.K., Verma, M.K., Ahmad, I., Baier, K., Jha, R., Azzam, R., 2016. Assessment of groundwater vulnerability using modified DRASTIC model in Kharun Basin, Chhattisgarh, India. Arab. J. Geosci. 9 (2), 98.
Stigter, T.Y., Ribeiro, L., Dill, A.M.M.C., 2005. Evaluation of an intrinsic and a specific vulnerability assessment method in comparison with groundwater salinization and nitrate contamination levels in two agricultural regions in the south of Portugal. Hydrogeol. J. 14 (1–2), 79–99.
Tabatabaei, S.H., Khoshdooz, N., Babazadeh, H., Hosseinipour, E.Z., Shirani, M., Jamali, B., Talebi, L., 2014. Assessment of groundwater vulnerability in a coastal region using DRASTIC and IM-DRASTIC models: case study of Kish Island, Iran. In: World Environmental and Water Resources Congress 2014, pp. 252–261.
Tiwari, A.K., Singh, P.K., De Maio, M., 2016. Evaluation of aquifer vulnerability in a coal mining of India by using GIS-based DRASTIC model. Arab. J. Geosci. 9 (6), 438.
USGS, 2000. Is Seawater Intrusion Affecting Ground Water on Lopez Island, Washington? *USGS Fact Sheet*. 057-00. Department of the Interior; U.S. Geological Survey, Tacoma, Washington.
Vías, J.M., Andreo, B., Perles, M.J., Carrasco, F., Vadillo, I., Jiménez, P., 2006. Proposed method for groundwater vulnerability mapping in carbonate (karstic) aquifers: the COP method. Hydrogeol. J. 14 (6), 912–925.
Vlaicu, M., Munteanu, C.-M., 2008. Karst Groundwaters Vulnerability Assessment Methods. Emile Racovitza Institute of Speology, Romania.
Voigt, H.-J., Heinkele, T., Jahnke, C., Wolter, R., 2004. Characterization of groundwater vulnerbaility to fulfill requirements of the water framework directive of the European Union. Geoffisca Int. 43 (4), 567–574.
Vorosmarty, C.J., Green, P., Salisbury, J., Lammers, R.B., 2000. Global water resources: vulnerability from climate change and population growth. In: Science. vol. 289. American Association for the Advancement of Science, pp. 284–288.
Wagner, Richard J., Boulger Jr., Robert W., Oblinger, Carolyn J., Smith, B.A., 2006. Guidelines and Standard Procedures for Continuous Water-Quality Monitors: Station Operation, Record Computation, and Data Reporting. U.S. Geological Survey Techniques and Methods 1–D3 Department of the Interior and U.S. Geological Survey, Reston, Virginia.
Walley, C., 1997. The Lithostratigraphy of Lebanon. Lebanese Sci. Bull. 10 (1).
Werner, A.D., Ward, J.D., Morgan, L.K., Simmons, C.T., Robinson, N.I., Teubner, M.D., 2012. Vulnerability Indicators of Sea Water Intrusion. Ground Water 50 (1), 48–58.
WHO, 2003. Chloride in Drinking-Water. *Background Document for Development of WHO Guidelines for Drinking-Water Quality*. Guidelines for Drinking-water Quality. World Heatlh Organization, Geneva, Switzerland.
Yang, J., Tang, Z., Jiao, T., Muhammad, A.M., 2017. Combining AHP and genetic algorithms approaches to modify DRASTIC model to assess groundwater vulnerability: a case study from Jianghan Plain, China. Environ. Earth Sci. 76 (12), 426.
Yin, L., Zhang, E., Wang, X., Wenninger, J., Dong, J., Guo, L., Huang, J., 2013. A GIS-based DRASTIC model for assessing groundwater vulnerability in the Ordos Plateau, China. Environ. Earth Sci. 69 (1), 171–185.
Zghibi, A., Merzougui, A., Chenini, I., Ergaieg, K., Zouhri, L., Tarhouni, J., 2016. Groundwater vulnerability analysis of Tunisian coastal aquifer: an application of DRASTIC index method in GIS environment. Groundw. Sustain. Dev. 2–3, 169–181.